

THE EFFECTS OF RADIATIVE COOLING ON THE ENTROPY DISTRIBUTION OF INTRACLUSTER GAS

IAN G. McCARTHY, MARK A. FARDAL, AND ARIF BABUL

Department of Physics & Astronomy, University of Victoria, Victoria, BC, V8P 1A1, Canada;
 imccarth@uvic.ca, fardal@uvic.ca, babul@uvic.ca

Draft version November 7, 2018

ABSTRACT

High resolution X-ray observations indicate that the entropy profiles in the central regions of some massive cooling flow clusters are well approximated by powerlaws. McCarthy and coworkers recently accounted for this trend with an analytic model that includes the detailed effects of radiative cooling. Interestingly, these authors found that cooling (and subsequent inflow of the gas) *naturally* establishes approximate steady-state powerlaw entropy profiles in the cores of clusters. However, the origin of this behavior and its dependence on initial conditions have yet to be elucidated. In the present study, we explain this trend in the context of the self-similar cooling wave model developed previously by Bertschinger (1989). It is shown that the logarithmic slope of the entropy profile in the cores of relaxed cooling flow clusters is given by a simple analytic function that depends only on the logarithmic slopes of the local gravitational potential and the cooling function. We discuss a number of potentially interesting uses of the above result, including: (1) a way of measuring the shapes of gravitational potentials of cooling flow clusters (which may, for example, be compared against the standard hydrostatic equilibrium method); (2) a simple method for constructing realistic analytic cluster models that include the effects of radiative cooling; and (3) a test of the reliability of cooling routines implemented in analytic models and hydrodynamic simulations.

Subject headings: cosmology: theory — galaxies: clusters: general — X-rays: galaxies: clusters

1. INTRODUCTION

The presence of strong positive temperature gradients (e.g., Allen et al. 2001; De Grandi & Molendi 2002; Piffaretti et al. 2004; Vikhlinin et al. 2004) and the lack of an obvious entropy floor (e.g., Pratt & Arnaud 2002; Mushotzky et al. 2003; Piffaretti et al. 2004) in the cores of some clusters have stimulated interest in theoretical models of the intracluster medium (ICM) that include the effects of radiative cooling. Such models have been shown to be in broad agreement with the current suite of X-ray observations of clusters, particularly if some form of feedback/heating is also incorporated into the models (e.g., Tozzi & Norman 2001; Voit et al. 2002; Oh & Benson 2003; Borgani et al. 2004; McCarthy et al. 2004, hereafter M04).

Interestingly, by assembling published *Chandra* and *XMM-Newton* X-ray data from the literature, M04 uncovered a population of relaxed clusters (e.g., A2029, PKS0745, Hydra A) with central entropy profiles (where we define the “entropy”, S , as $kTn_e^{-2/3}$) that are well approximated by powerlaws (see also the recent study of Piffaretti et al. 2004). M04 were able to account for these clusters (as well as other clusters that exhibit large entropy cores) with a simple analytic model that includes the detailed effects of cooling and that assumes the ICM was initially heated prior to cooling. In particular, M04 found that if the ICM in a given cluster is initially heated¹ by only a mild amount, cooling *naturally*

establishes approximate powerlaw entropy profiles near the cluster core². It would be interesting to understand from a physical perspective what is driving this trend in the observed and model clusters.

Unfortunately, a rigorous calculation of the effects of radiative cooling and the subsequent (quasi-hydrostatic) inflow of intracluster gas can only formally be obtained by numerically solving the time-dependent hydrodynamic equations (as approximately done, e.g., in M04). This makes it a challenge to understand physically why the above trends are established by cooling. Despite this inconvenience, there are, however, analytic tools at our disposal that can help to establish a physical picture. For example, Bertschinger (1989) (hereafter, B89) used a self-similarity analysis to derive the behavior of cooling flows in clusters. One of the interesting results derived by Bertschinger is that the logarithmic slopes of the gas density and temperature profiles in the limit $r \ll r_{cool}$ (where r_{cool} is the radius at which the cooling time of the gas equals the age of the cluster) depend only on the shapes of the cluster gravitational potential and of the cooling function, $\Lambda(T)$. The behavior of the gas density and temperature profiles can be used to infer how radiative cooling influences the distribution of intracluster entropy, which is perhaps a more fundamental quantity since convection will strive to prevent the establishment of a rising entropy profile towards the cluster center (see, e.g., Voit et al. 2002). Thus, the study of B89 is a good starting point for our investigation of the effects of cooling and inflow on intracluster entropy.

In the present study, we briefly review the self-similar analysis of B89, including the basic assumptions made in that study and their validity, and use his results to derive how radiative cooling modifies the entropy profiles of clusters. We compare the self-similar solution to the

¹ We note that such “preheating” does not preclude subsequent heating events following cluster formation, such as AGN feedback initiated by the accretion of cold gas at the cluster center.

² However, the mild amount of heating is sufficient to delay the onset of catastrophic cooling for up to several Gyr and, as a result, the predicted global cold gas fractions remain consistent with observationally established limits.

results of the 1-D cooling model of M04 for clusters with powerlaw dark matter profiles and that cool via thermal bremsstrahlung and, indeed, find extremely good agreement in the limit $r \ll r_{cool}$. We further demonstrate that the self-similar solution should provide an accurate description for cooling (via both bremsstrahlung *and* line emission) in more realistic dark matter halos. Finally, we discuss a number of interesting uses of this result, including measuring the shapes of cluster gravitational potentials (that, e.g., could be compared against the usual hydrostatic equilibrium method), testing the reliability of numerical cooling routines in analytic models and hydro simulations, and as a simple way of setting up initial conditions for cluster models with radiative cooling.

2. COOLING FLOWS AND SELF-SIMILARITY: THE BERTSCHINGER SOLUTION

As noted above, in general, the time-dependent hydrodynamic equations must be solved numerically in order to obtain a detailed picture of the effects of radiative cooling on cluster gas. However, when the time dependence is due to a single physical process that can be characterized by a unique scale length [in this case, the cooling radius³, $r_{cool}(t)$], similarity solutions can provide useful physical insight. Adopting this approach, B89 derived the general behavior of cooling flows in clusters of varying gravitational potentials (and with varying cooling functions as well). We are especially interested in the properties of his solution in the limit $r \ll r_{cool}$, since they are independent of the initial conditions of the gas. (Outside the cooling radius the initial conditions are of crucial importance since radiative cooling hasn't had enough time to significantly modify the gas there.) Before examining the solution itself, let us first review the basic assumptions made in B89 and their validity.

Since self-similar solutions can be characterized by only a single scale length, some simplifying assumptions are required in order to obtain a solution for the properties of cooling flows. In particular, Bertschinger assumed that the gravitational potential and the cooling function could be characterized by simple powerlaws that remained fixed as a function of time. Of course, in reality, neither of these assumptions are strictly valid. High resolution numerical simulations indicate that the dark matter density profiles of clusters (and halos of other masses as well) have a characteristic scale length (the so-called scale radius, r_s), where the index of the powerlaw profile changes from relatively shallow (between ~ -1 and -1.5 ; e.g., Navarro, Frenk, & White (NFW) 1997; Moore et al. 1999) to relatively steep (~ -3). The cooling function is not scale-free either, owing primarily to line emission. Thus, one is justified in questioning the physical relevance of a model that invokes these assumptions. (However, physical relevance may not be of major concern if one is simply testing the reliability of numerical cooling methods.) We examine in §3.2 whether relaxing these assumptions significantly affects the shapes of the resulting entropy profiles in the cores of *massive* clusters.

³ The cooling radius grows larger with time. Unfortunately, the self-similar solution in B89 is expressed in terms of the *initial* cooling radius. Thus, it might be expected that comparison to observations, which are used to infer the *present* cooling radius, is somewhat ambiguous. However, as highlighted by B89, this leads to only a small error since, over the course of a cluster's life, the cooling radius grows only by a small amount.

Other assumptions made in the analysis of B89 include spherical symmetry, subsonic inflow, and single-phase cooling. Spherical symmetry is expected to be approximately valid, at least in an average sense for a reasonably large relaxed cluster sample. Likewise, subsonic flow should hold for the majority of the gas within r_{cool} , except possibly near the very center where the gas may become transsonic. However, it has yet to be determined whether or not multi-phase cooling is important in clusters. In the absence of significant non-gravitational heating, the intracluster gas *is* thermally unstable. However, because the gas flows into the cluster center essentially as fast as it cools, we expect multi-phase cooling to be important only near the very center (see B89). Recent spatially-resolved *Chandra* and *XMM-Newton* spectra of the central regions cooling flow clusters have confirmed that, probably with the exception of the very central radial bin, single-phase models provide at least as good a fit as multi-phase models (e.g., David et al. 2001; Matsushita et al. 2002). For the present study, we assume single-phase cooling.

Finally, it is implicitly assumed that there are no significant sources of non-gravitational heating (such as AGN feedback, thermal conduction, and turbulent mixing) present in the ICM. In §4, we give a brief discussion of the potential impact of such heating.

Implementing the above assumptions, B89 renormalized the hydrodynamic equations by removing any time dependence arising through $r_{cool}(t)$. A self-similar solution is obtained if one neglects the acceleration terms (which is valid since the inflow of gas is highly subsonic) in the renormalized hydro equations. It is straightforward to derive the limiting behavior of the gas density and temperature profiles in the limit $r \ll r_{cool}$ under these conditions (see eqns. 2.30 of B89):

$$\frac{d \log \rho}{d \log r} = \frac{-3 + (2 - \alpha)(1 - \beta)}{2}, \quad \frac{d \log T}{d \log r} = 2 - \alpha \quad (1)$$

where we have assumed that dark matter dominates the gravitational potential and that $\rho_{dm} \propto r^{-\alpha}$ and $\Lambda(T) \propto T^\beta$. Note that the definitions of α and β differ from the definitions of these symbols in B89.

In §1, we defined the “entropy”, S , in terms of gas density and temperature. The above equations can, therefore, be used to yield the logarithmic slope of the entropy profile within r_{cool} :

$$\gamma \equiv \frac{d \log S}{d \log r} = \left[1 - \frac{1}{3}(1 - \beta) \right] (2 - \alpha) + 1 \quad (2)$$

Thus, for $\beta = 1/2$ (i.e., cooling dominated by thermal bremsstrahlung),

$$\gamma = \frac{5}{6}(2 - \alpha) + 1 \quad (3)$$

which yields $\gamma = 1$ for a singular isothermal sphere ($\alpha = 2$), $\gamma \approx 1.4$ for a Moore et al. profile in the limit $r \ll r_s$ ($\alpha = 1.5$), and $\gamma \approx 1.8$ for a NFW profile in the limit $r \ll r_s$ ($\alpha = 1$). Note, however, that the value of γ in equation (2) depends only weakly on the shape of the cooling function (that is, for reasonable values of β ranging from $-1/2$ to $1/2$) for $\alpha \gtrsim 1$.

Below, we compare this simple analytic result with the 1-D cooling model of M04.

3. COMPARISON WITH M04

3.1. Powerlaw clusters

M04 developed a simple radiative cooling code which, when applied to the entropy injection model clusters of Babul et al. (2002), successfully and simultaneously reproduces the luminosity-temperature and luminosity-mass relations (including their associated intrinsic scatter) and yields detailed fits to the entropy, surface brightness, and temperature profiles of clusters as inferred from recent high resolution X-ray observations. As alluded to in §1, these authors found that radiative cooling established a powerlaw entropy profile in cores of their model clusters that experienced only mild preheating (that is, for those clusters that were initially injected with $\lesssim 300$ keV cm 2 , i.e., the entropy cooling threshold for massive clusters). It is interesting to see whether or not this trend can be explained by the self-similar solution of B89.

In order to test this, we use the model of M04 (see §2.2 of M04 for a detailed discussion of the model) to track the effects of cooling for a set of clusters with arbitrary initial conditions (recall that the solution of B89 within the cooling radius does not depend on initial gas conditions). For specificity, however, we show results for clusters that have a total dark matter mass of $10^{15} M_{\odot}$, a total gas mass of $\approx 1.5 \times 10^{14} M_{\odot}$, and a maximum radius, r_{halo} , of 2.06 Mpc. The cluster gas is initially assumed to be in hydrostatic equilibrium within a dark matter halo that is characterized by a density profile $\rho_{dm} \propto r^{-\alpha}$ (the normalization being set by the mass and radius given above). The cluster gas is then allowed to evolve via radiative cooling and inflow until a stable entropy profile is achieved. To calculate the cooling rate, we assume a cooling function that scales as $\Lambda(T) \propto T^{1/2}$ with a normalization that is set by matching a zero metallicity Raymond-Smith plasma at a temperature of $T \approx 10^8$ K. Finally, as in M04, we remove any gas that is able to cool below a threshold temperature of 10^5 K from the calculation and assume that its dynamical effects on the cluster gravitational potential are negligible. Clearly, if a significant amount of gas is able to completely cool this assumption will be violated. However, in this case, we expect these effects will be relevant only for the central tens of kpc and will have only a minor effect on the overall entropy distribution within the cooling radius.

To show how the effects of cooling are linked to the underlying gravitational potential, we present Figure 1. Focusing first on the top left-hand panel, we start with a cluster that is initially characterized by entropy profile that contains a core and a logarithmic slope of $\gamma = 1.1$ outside the core. This is the initial slope adopted by Babul et al. (2002) and M04 and is what one expects if the gas is in hydrostatic equilibrium and if its density profile traces that of the dark matter (e.g., Voit et al. 2002; Williams et al. 2004), an expectation that is supported by high resolution hydrodynamic simulations (e.g., Lewis et al. 2000; Voit et al. 2003; Ascasibar et al. 2003; Voit 2004). As can be clearly seen, the slope of the dark matter profile, α , is important in determining the resulting slope of the entropy profile, γ , within $0.1r_{\text{halo}}$ (which corresponds roughly to r_{cool} for these clusters). In particular, as the dark matter profile steepens the resulting entropy profile becomes more shallow, agreeing qualitatively and quantitatively with equation (3).

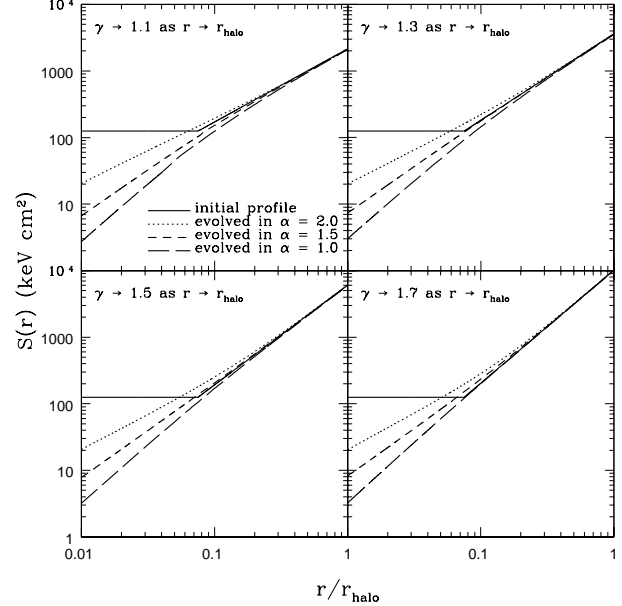


FIG. 1.— The effects of cooling and inflow on the entropy distribution of clusters. Solid lines represent the initial entropy profiles. The dotted, short dashed, and long dashed lines represent the resulting steady-state entropy profiles when the clusters are evolved in dark matter halos that have density profiles characterized by powerlaw indices of $\alpha = 2.0$, 1.5 , and 1.0 , respectively. The various panels show the resulting profiles for different initial entropy distributions. Figure 2 presents a comparison of the central logarithmic entropy slopes to the Bertschinger solution.

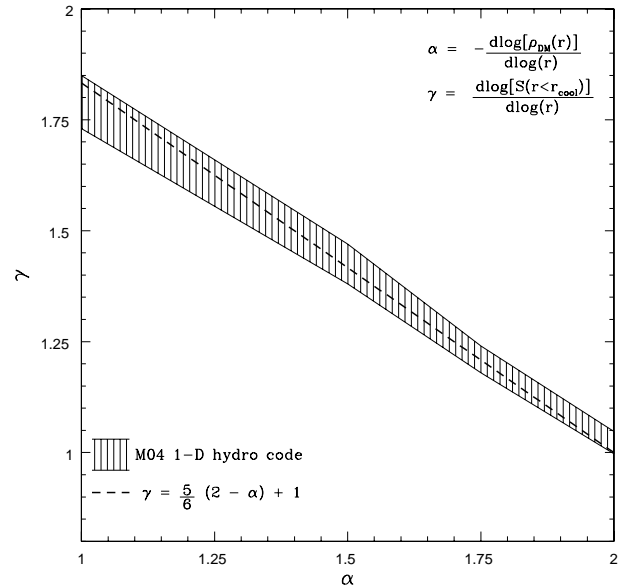


FIG. 2.— Comparison of the self-similar solution of B89 with the results of M04's cooling model. The shaded region reflects the uncertainty in the best fit powerlaw indices of the entropy profiles (within r_{cool}) shown in Fig. 1.

The remaining panels of Figure 1, which show the results for clusters that initially have steeper entropy profiles outside the entropy core, illustrate that the initial gas conditions of the clusters have almost no effect on the resulting steady-state entropy profile within r_{cool} . Like-

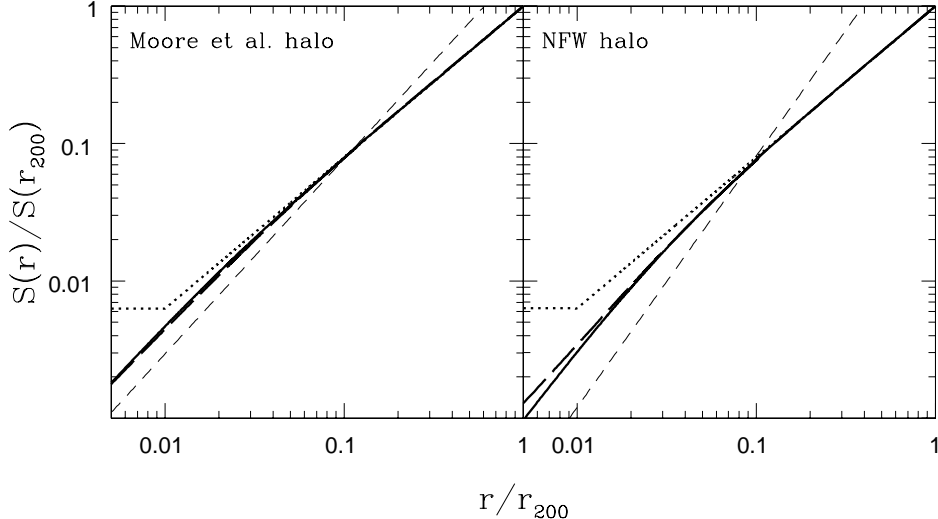


FIG. 3.— The effects of line emission and realistic dark matter profiles on the steady-state entropy profile. *Left:* A cluster with a Moore et al. dark matter halo. *Right:* A cluster with an NFW dark matter halo. In both panels the dotted line represents the initial entropy distribution, the thick solid lines represent the final entropy distribution assuming cooling with a pure thermal bremsstrahlung cooling function, and the thick dashed lines represent the final entropy distribution assuming cooling with a Raymond-Smith plasma model with $Z = 0.3Z_{\odot}$. The thin dashed lines indicate the slope predicted by B89's self-similar model assuming $\beta = 1/2$ and $\alpha = 1.5$ (left panel) and $\alpha = 1.0$ (right panel). They have been arbitrarily normalized to cross the thick lines at the cooling radius.

wise, what happens in the interior of the cluster does not significantly influence gas outside of r_{cool} , as expected.

We have fitted the entropy profiles within r_{cool} with powerlaws. However, we find that the entropy profiles within r_{cool} are not *exact* powerlaws and there is some “wiggle” room in the best fit logarithmic slope, depending on the range of radii over which the profiles are fitted. For example, the best fit logarithmic slope over the range $0 \leq r \leq r_{cool}/2$ differs slightly from the best fit over the range $r_{cool}/2 \leq r \leq r_{cool}$. We use these two radial intervals to roughly quantify the scatter in the best fit slope. Figure 2 presents a comparison between the analytic self-similar solution of B89 and the fits to the entropy profiles shown in Fig. 1. The shaded region roughly reflects the uncertainty in the best fit powerlaw indices for the profiles predicted by M04’s cooling model.

Reassuringly, excellent agreement between the self-similar solution and the 1-D cooling code is obtained. Thus, the self-similar cooling wave model of B89 provides a physical basis for the powerlaw trends found by M04. In addition, the agreement in Figure 2 gives us confidence in the reliability of the 1-D cooling model developed in M04.

3.2. Realistic clusters

Observed clusters and clusters formed in cosmological numerical simulations do not have pure powerlaw gravitational potentials. Furthermore, the ICM contains a significant quantity of metals and, consequently, cools not only through thermal bremsstrahlung but also through line emission. Line emission has the effect of distorting the cooling function away from the powerlaw form that is characteristic of bremsstrahlung. For these two reasons, the physical relevance of the results presented in §3.1 may be questioned. Below, we investigate the ex-

tent to which the shape of the resulting entropy profile is affected by these assumptions.

Since we are introducing additional scales into the problem, it is important that we construct realistic cluster models. We consider two different systems: one with a NFW dark matter profile and one with a Moore et al. dark matter profile. Both systems have been chosen to have the same total gas and dark matter masses; specifically, $M_{gas}(r_{200}) \approx 1.5 \times 10^{14} M_{\odot}$ and $M_{dm}(r_{200}) = 10^{15} M_{\odot}$, where $r_{200} \approx 2.06$ Mpc. We use a typical cluster dark matter concentration of $c_{\text{NFW}} \equiv r_{200}/r_s \approx 3.4$ for the NFW halo (e.g., Eke et al. 1998; Bullock et al. 2001) and $c_{\text{Moore}} \equiv r_{200}/r_{(-2)} = c_{\text{NFW}}/0.630 \approx 5.4$ for the Moore et al. halo (see Keeton 2001). The above implies a scale radius, r_s , of ≈ 600 kpc. As for the intracluster gas, we turn to the studies of Voit et al. (2003) and Voit (2004). These authors found that the entropy profiles of a large sample of clusters generated with a numerical simulation of a Λ CDM cosmology including hydrodynamics (e.g., shock heating) but not radiative cooling are approximately self-similar over a wide range of masses (see Fig. 11 of Voit 2004). The initial entropy distributions of our model clusters are assumed to be identical to Voit’s best fit to his simulated clusters⁴. The initial gas density and temperature distributions are determined through the equation of hydrostatic equilibrium by applying the boundary condition that the total amount of gas within r_{200} is equal to that specified above.

⁴ At large radii, i.e., for $r > 0.1r_{200}$, Voit (2004) reports a best fit entropy profile of $S(r) \propto r^{1.1}$. At small radii, however, there is an apparent entropy core whose origin remains uncertain. We have shrunk this core for computational convenience, since the model clusters reach steady state more quickly if they have small initial entropy cores. However, this modification does not affect our results or conclusions since the entropy core is contained entirely

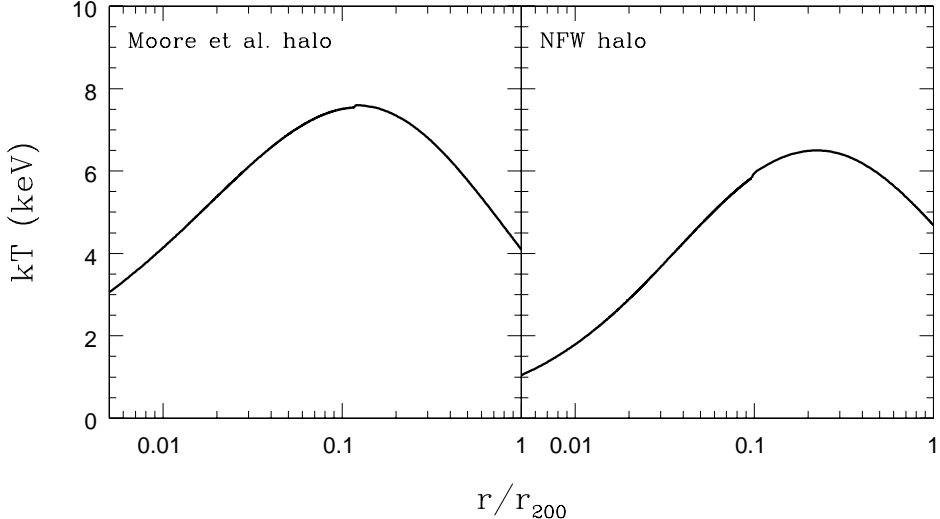


FIG. 4.— The final (steady-state) temperature distributions of the gas in the Moore et al. and NFW halos.

To compute the effects of cooling, we again make use of the model developed by M04. In order to gauge the effects of line emission, we explore two different cooling functions: the pure thermal bremsstrahlung function implemented in §3.1 and a Raymond-Smith plasma with a metallicity set to $0.3Z_{\odot}$. As in the case of the powerlaw models, we neglect the dynamical effects of mass drop out and we run the cooling model until steady-state entropy profiles are achieved. At steady state, we find that both clusters have similar global emission-weighted temperatures with $kT_{ew} \approx 5$ keV.

In Figure 3, we plot the initial and final entropy profiles of our model clusters. In both panels, the dotted lines represent the initial entropy distributions, the thick solid lines represent the final distributions when cooled using a pure bremsstrahlung cooling function, and the thick dashed lines represent the final distributions when cooled using the $0.3Z_{\odot}$ Raymond-Smith plasma cooling function. The thin dashed lines indicate the slope predicted by B89’s self-similar model assuming $\beta = 1/2$ and $\alpha = 1.5$ (left panel) and $\alpha = 1.0$ (right panel). They have been arbitrarily normalized to cross the thick lines at the cooling radius.

First, consider the role of the cooling function. For the Moore et al. halo, there is virtually no dependence on which cooling function we use. The resulting entropy distribution for the NFW halo, however, is slightly shallower if we include line emission. This difference can be understood as follows. The gravitational potential of the Moore et al. halo is steeper than that of the NFW halo. Consequently, gas flowing into the center of the Moore et al. halo requires more thermal support to remain in hydrostatic equilibrium. In Figure 4, we plot the final (steady-state) temperature distributions of the two model clusters. Note that the central temperature of the

within the cooling radius. As discussed above, the resulting *steady-state* entropy profile within r_{cool} depends only on the shapes of the gravitational potential and the cooling function (and not on the initial properties of the gas within r_{cool}).

Moore et al. halo is roughly 3 times larger than that of the NFW halo. In Figure 5, we show the cooling function for a Raymond-Smith plasma with $Z = 0.3Z_{\odot}$. For temperatures of $kT \gtrsim 2$ keV, the cooling function is dominated by thermal bremsstrahlung and is well approximated by a powerlaw; $\Lambda(T) \propto T^{1/2}$. This then explains why the entropy profile of the Moore et al. halo is unaffected by line emission: at any particular time there is virtually no gas below 2 keV (except at the exact center where gas rapidly cools below the X-ray emitting threshold of $\approx 10^5$ K). The shallower NFW potential, however, permits some gas to cool below 2 keV before reaching the center of the cluster. The thin dotted line in Fig. 5 shows the best fit powerlaw to the cooling function between $0.1 \text{ keV} \leq kT \leq 2 \text{ keV}$, which has an index of $\beta \approx -0.35$. Using this value for β in equation (2), we are able to account for the slight ($\sim 10\%$) deviation in the shape of the entropy profile within the central $0.01r_{200}$ (≈ 20 kpc) of the NFW halo.

The shape of the final entropy profile is more sensitive to the shape of the gravitational potential than it is to the shape of the cooling function. Thus, we might expect self-similar solution to be a poor description of the final shape of entropy profiles in realistic dark matter halos. However, the left hand panel of Fig. 3 demonstrates that the shape of final entropy profile of the Moore et al. halo (thick lines) is virtually identical to that of a halo with a pure powerlaw profile of $\alpha = 1.5$ (thin dashed line). Likewise, with the exception of the small deviation at the center due to line emission, the shape of the entropy profile in the NFW halo is essentially identical to that of a halo with a pure powerlaw profile of $\alpha = 1.0$ (see right hand panel of Fig. 3). Recall that in the limit of $r \ll r_s$, the logarithmic slopes of the Moore et al. and NFW halos asymptote to $\alpha = 1.5$ and 1.0 , respectively. Fig. 3 illustrates that what is relevant is the shape of the *local* gravitational potential (i.e., at $r \lesssim r_{cool}$), not the shape of the overall potential. Thus, the self-similar

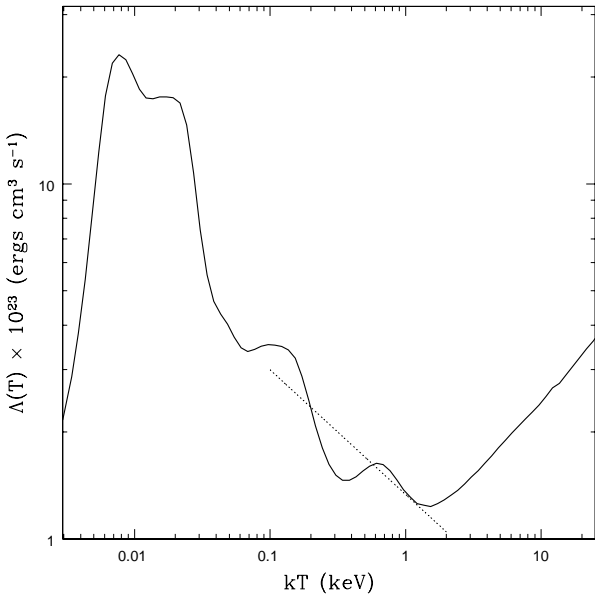


FIG. 5.— The cooling function for a Raymond-Smith plasma with $Z = 0.3Z_{\odot}$. The dotted line represents the best fit powerlaw (with $\beta \approx -0.35$) to the function over the range $0.1 \text{ keV} \leq kT \leq 2.0 \text{ keV}$.

solution provides an excellent description of steady-state cooling entropy profiles in realistic clusters *so long as the cooling radius is smaller than the cluster's scale radius*. This condition should be met for most high mass clusters as the typical cooling radius of clusters is of order $\sim 100-200$ kpc (e.g., Peres et al. 1998), while the typical dark matter scale radius of massive clusters in high resolution cosmological simulations is of order $\sim 400-700$ kpc (e.g., Eke et al. 1998; Bullock et al. 2001).

We conclude that the self-similar solution of B89 should provide a good description of the shapes of entropy profiles (for $r \lesssim r_{cool}$) of massive clusters that cool via thermal bremsstrahlung and line emission and that have realistic dark matter profiles. The reason for this is that self-similarity is only mildly violated for high mass clusters. The deep gravitational potential wells of massive clusters ensure that most of the intracluster medium is quite hot ($kT \gtrsim 2$ keV), even within the cooling radius, and thus thermal bremsstrahlung (which is scale-free) dominates the X-ray emissivity. The potential wells themselves have a characteristic scale radius but, for massive clusters, this radius is typically much larger than the cooling radius. Therefore, the central cooling flow essentially “feels” only a pure powerlaw potential (as assumed by B89).

4. DISCUSSION

Using the self-similar solution of B89, we have shown that radiative cooling and inflow lead to a characteristic entropy profile within the cooling radius that depends only on the shapes of the cooling function and the gravitational potential. We have compared the self-similar solution to the cooling model of M04 and, reassuringly, find excellent agreement for clusters with powerlaw potentials and that cool via thermal bremsstrahlung. Furthermore, we have demonstrated that the self-similar so-

lution is also valid for more realistic dark matter potentials and cooling functions that include line emission, at least for massive clusters where bremsstrahlung dominates line emission and the typical dark matter scale radius is much larger than the cooling radius. This result explains the numerically-derived trends found in M04, which provide a good fit to a number of observed cooling flow clusters. Kaiser & Binney (2003) have also recently reported that cooling establishes a powerlaw trend between ICM gas mass and entropy. This trend is also likely to be explained by the self-similar solution.

The self-similar model of B89 implicitly assumes that there are no significant sources of non-gravitational heating present in the ICM. Heating introduces an additional scale into the problem and, potentially, violates self-similarity. It is clear, however, that some form of heating has (or is) occurred in real clusters in order to prevent the so-called cooling crisis (see Balogh et al. 2001). Additional evidence for heating comes from recent high resolution *Chandra* images of many cooling flow clusters that reveal buoyantly-rising bubbles of hot plasma (e.g., Heinz et al. 2002; Blanton et al. 2003). These bubbles were presumably blown by a central AGN and must be heating the ICM at some level. Other sources of heating, such as thermal conduction (e.g., Medvedev & Narayan 2001) and stirring due to the orbital motions of cluster galaxies (e.g., El-Zant et al. 2004), are also a possibility. The relevant questions therefore are: (i) Is the level of heating sufficiently high to severely violate self-similarity? (ii) If so, is the heating distributed or restricted to only the very center of the cluster? (iii) In the event the heating is episodic (such as AGN heating), when did the last heating episode occur (i.e., has enough time passed in order to approximately re-establish a self-similar cooling flow)? A number of relaxed clusters with published entropy profiles show evidence for large entropy cores (M04). Clearly, such systems cannot be explained by the present self-similar cooling model, as these clusters were severely heated and the heating was distributed to large radii. However, M04 (see also Piffaretti et al. 2004) also found that several massive cooling flow clusters (e.g., A2029, PKS0745, Hydra A) have nearly pure powerlaw entropy profiles (except perhaps at very small radii, $r \lesssim 30$ kpc). This likely indicates that the self-similar model provides a reasonably accurate description of the cooling gas in this particular subset of observed clusters.

A test of the above hypothesis is to infer the slopes of the gravitational potentials of these clusters by using the slopes of their observed entropy profiles together with equation (3). This may then be compared with the results obtained using the standard hydrostatic equilibrium method for inferring the gravitational potential of clusters. Making use of the clusters with powerlaw entropy profiles from M04 (A2029, PKS0745, Hydra A), we find that the logarithmic slopes of their total matter density (dark matter and baryons) profiles are relatively steep, with $1.3 \lesssim \alpha \lesssim 2$. This agrees quite well with the recent hydrostatic analysis of *Chandra* data of 10 relaxed cooling flow clusters by Arabadjis & Bautz (2004). Thus, for this small sample of clusters, the self-similar model appears to provide an apt description of the cooling gas in the centers of these clusters. A more detailed comparison will soon be possible as the number of published

cluster entropy profiles is rapidly increasing.

Quite independent of how well it describes observed clusters, the self-similar model also has a number of interesting *theoretical* uses. We briefly discuss but two here.

1.) A simple method for calculating initial conditions of analytic model clusters with radiative cooling. This could serve as a “poor man’s alternative” to a model that explicitly takes into account the effects of radiative cooling and inflow on intracluster gas. For example, a realistic set of initial conditions could be generated by using the results of non-radiative simulations (e.g., Lewis et al. 2000; Loken et al. 2002; Voit 2004) to describe the gas at large radii ($r > r_{cool}$) while using the self-similar solution of B89 to describe the properties of the gas within r_{cool} . The normalization of the entropy profile within r_{cool} (which is not specified by the self-similar solution) could be set by matching the non-radiative simulation results near r_{cool} . One example of where such initial conditions might be useful is for models that explore the ability of various heating mechanisms to offset radiative losses of the ICM. For example, a number of recent AGN heating simulations (e.g., Quilis, Bower, & Balogh 2001; Ruszkowski & Begelman 2002) have invoked initial conditions such as isothermality or temperature profiles derived from non-radiative simulation (as opposed to that

expected for a cluster that is cooling radiatively) and this may have some effect on the estimates of the energetic requirements for the prevention of catastrophic cooling. It would be interesting to see whether the estimates of the amount of required heating change significantly when more realistic initial conditions (such as those proposed above) are implemented.

2.) A test of the reliability of cooling routines implemented in analytic models and hydrodynamic simulations. Because the self-similar solution is a simple function, it can easily be used to test, for example, how well various formulations of smoothed particle hydrodynamics (SPH) or mesh-based techniques [such as adaptive mesh refinement (AMR)] treat the effects of cooling (see, e.g., Abadi, Bower, & Navarro 2001). We are currently undertaking such a study using a variety of popular analytic and hydrodynamic codes (Dalla Vecchia et al. in preparation).

I. G. M. is supported by a postgraduate scholarship from the Natural Sciences and Engineering Research Council of Canada (NSERC) and A. B. is supported by an NSERC Discovery Grant. A. B. would also like to acknowledge support from the Leverhulme Trust (UK) in the form of the Leverhulme Visiting Professorship.

REFERENCES

Abadi, M. G., Bower, R. G., & Navarro, J. F. 2000, MNRAS, 314, 759

Allen, S. W., Schmidt, R. W., & Fabian A. C. 2001, MNRAS, 328, L37

Arabadjis, J. S., & Bautz, M. W. 2004, ApJ, submitted (astro-ph/0408362)

Ascasibar, Y., Yepes, G., Müller, V., & Gottlöber, S. 2003, MNRAS, 346, 731

Babul, A., Balogh, M. L., Lewis, G. F., & Poole, G. B. 2002, MNRAS, 330, 329

Balogh, M. L., Pearce, F. R., Bower, R. G., & Kay, S. T. 2001, MNRAS, 326, 1228

Bertschinger, E. 1989, ApJ, 340, 666 (B89)

Blanton, E. L., Sarazin, C. L., & McNamara, B. R. 2003, ApJ, 585, 227

Borgani, S., et al. 2004, MNRAS, 348, 1078

Bullock, J. S., et al. 2001, ApJ, 550, 21

David, L. P., et al. 2001, ApJ, 557, 546

De Grandi, S., & Molendi, S. 2002, ApJ, 567, 163

Eke, V. R., Navarro, J. F., & Frenk, C. S. 1998, ApJ, 503, 569

El-Zant, A., Kim, W.-T., & Kamionkowski, M. 2004, MNRAS, 354, 169

Heinz, S., Choi, Y.-Y., Reynolds, C. S., & Begelman, M. C. 2002, ApJ, 569, L79

Kaiser, C. R., & Binney, J. 2003, MNRAS, 338, 837

Keeton, C. R. 2001, ApJ, 561, 46

Lewis, G. F., Babul, A., Katz, N., Quinn, T., Hernquist, L., & Weinberg, D. H. 2000, ApJ, 536, 623

Loken, C., Norman, M. L., Nelson, E., Burns, J., Bryan, G. L., & Motl, P. 2002, ApJ, 579, 571

Matsushita, K., Belsole, E., Finoguenov, A., & Böhringer, H. 2002, A&A, 386, 77

McCarthy, I. G., Balogh, M. L., Babul, A., Poole, G. B., & Horner, D. J. 2004, ApJ, 613, 811 (M04)

Moore, B., Quinn, T., Governato, F., Stadel, J., & Lake, G. 1999, MNRAS, 310, 1147

Mushotzky, R., Figueroa-Feliciano, E., Loewenstein, M., & Snowden, S. L. 2003, ApJ, submitted

Narayan, R., & Medvedev, M. V. 2001, ApJ, 562, L129

Navarro, J. F., Frenk, C. S., & White, S. D. M. 1997, ApJ, 490, 493

Oh, S. P., & Benson, A. J. 2003, MNRAS, 342, 664

Peres, C. B., Fabian, A. C., Edge, A. C., Allen, S. W., Johnstone, R. M., & White, D. A. 1998, MNRAS, 298, 416

Piffaretti, R., Jetzer, Ph., Kaasstra, J. S., & Tamura, T. 2004, A&A, in press (astro-ph/0412233)

Pratt, G. W., & Arnaud, M. 2002, A&A, 394, 375

Quilis, V., Bower, R. G., & Balogh, M. L. 2001, MNRAS, 328, 1091

Ruszkowski, M., & Begelman, M. C. 2002, ApJ, 581, 223

Tozzi, P., & Norman, C. 2001, ApJ, 546, 63

Vikhlinin, A., Markevitch, M., Murray, S. S., Forman, W., & Van Speybroeck, L. 2004, ApJ, submitted (astro-ph/0412306)

Voit, G. M. 2004, Rev. Mod. Phys., in press (astro-ph/0410173)

Voit, G. M., Balogh, M. L., Bower, R. G., Lacey, C. G., & Bryan, G. L. 2003, ApJ, 593, 272

Voit, G. M., Bryan, G. L., Balogh, M. L., & Bower, R. G. 2002, ApJ, 576, 601

Williams, L. R. L., Austin, C., Barnes, E., Babul, A., & Dalcanton J. 2004. To appear in the Proceedings of Science, published by SISSA; Conference: “Baryons in Dark Matter Haloes”, Novigrad, Croatia, 5-9 October 2004; editors: R.-J. Dettmar, U. Klein, P. Salucci (astro-ph/0412442)